Neuroscience Letters 627 (2016) 168–177

Contents lists available at ScienceDirect

Neuroscience Letters

journal homepage: www.elsevier.com/locate/neulet

Research article

Reticulon 4A/Nogo-A influences the distribution of Kir4.1 but is not essential for potassium conductance in retinal Müller glia

Sandrine Joly[a,b,c], Dana A. Dodd[d], Benjamin F. Grewe[e], Vincent Pernet[a,b,c,*]

[a] CUO-Recherche, Médecine Régénératrice—Centre de recherche FRQS du CHU de Québec-Université Laval, Université Laval, Québec, Canada
[b] Centre de Recherche en Organogénèse expérimentale de l'Université Laval/LOEX, Québec, QC, Canada
[c] Département d'Ophtalmologie, Faculté de médecine, Université Laval, Québec, QC, Canada
[d] University of Texas Southwestern Medical Center, Department of Microbiology, Dallas, TX, USA
[e] Institute of Neuroinformatics, ETH Zurich, Zurich, Switzerland

HIGHLIGHTS

- The expression of Nogo-A is polarized in the radial Müller glia of the mouse retina.
- Virus-mediated Nogo-A upregulation enhances Kir4.1 immunoreactivity in Müller glia.
- Nogo-A and Kir4.1 interact in mouse retinae.
- Nogo-A gene deletion does not change potassium conductance in dissociated Müller glia.

ARTICLE INFO

Article history:
Received 20 May 2016
Received in revised form 2 June 2016
Accepted 4 June 2016
Available online 6 June 2016

Keywords:
Müller cells
Glia
Retina
Nogo-A
Kir4.1

ABSTRACT

In the adult retina, we have previously shown that Nogo-A was highly expressed in Müller glia. However, the role of Nogo-A in the glial cell physiology is not clear. In this study, we investigated the possible influence that Nogo-A may exert on other polarized molecules in Müller cells, in particular inwardly rectifying potassium channel 4.1 (Kir4.1) and aquaporin 4 (AQP4) that respectively control potassium and water exchange in glial cells. Our results showed that adenovirus-mediated Nogo-A overexpression with AdNogo-A increased the immunofluorescent signal of Kir4.1 in rat Müller cell line 1 (rMC-1) cells but did not change its expression level by Western blotting. *In vivo*, AdNogo-A induced ectopic Kir4.1 immunoreactivity throughout the radial processes of Müller cells compared with AdLacZ control virus. Surprisingly, AdNogo-A did not modify the distribution of Dp71 and AQP4 that are common binding partners for Kir4.1 in the dystrophin-associated protein (DAP) complex anchored at the plasma membrane of Müller glia. Immunoprecipitation experiments revealed molecular interactions between Nogo-A and Kir4.1. In Nogo-A KO mouse retinae, the distribution of Kir4.1 was not different from that observed in Wild-Type (WT) animals. In addition, potassium conductance did not change in freshly dissociated Nogo-A KO Müller glia compared with WT cells. In summary, the increase of Nogo-A expression can selectively influence the distribution of Kir4.1 in glia but is not essential for Kir4.1-mediated potassium conductance at the plasma membrane in physiological conditions. Nogo-A-Kir4.1 interactions may, however, contribute to pathological processes taking place in the retina, for instance, after ischemia.

1. Introduction

In the adult central nervous system (CNS), Nogo-A is a transmembrane protein essentially expressed by oligodendrocytes [1,2]. The inhibitory properties of Nogo-A on neuronal growth and plasticity have well been characterized in intact and injured regions of the CNS such as the spinal cord and the brain [3,4]. However, the role of Nogo-A in the physiology of adult glial cells is not clear. During development, we have previously observed that Nogo-A gene ablation delayed the maturation of oligodendrocytes [5]. In contrast, in adult mice deprived of Nogo-A (KO), the myelin sheath structure formed by mature oligodendrocytes appears normal [5,6]. The lack of phenotypic changes in KO animals may result from powerful compensatory mechanisms that have previously been

* Corresponding author at: CUO-Recherche, Université Laval Centre de recherche du CHU de Québec—Pavillon CHUL, 2705, Boul Laurier-Local P-09825, G1V 4G2 Québec, Canada.
E-mail address: vincent.pernet.1@ulaval.ca (V. Pernet).

http://dx.doi.org/10.1016/j.neulet.2016.06.010
0304-3940/

reported [7]. For example, repulsive guidance molecules are upregulated in Nogo-A KO mice [8]. Whether the physiology of glial cells is impaired in the adult CNS deprived of Nogo-A has not been studied yet.

Nogo-A expression is not limited to myelin-forming oligodendrocytes in the brain and in the spinal cord. In the retina, Nogo-A is enriched in the inner portion of Müller cell radial extension and in their so-called end-foot facing the vitreous body [9,10] (Fig. 1A). Müller cells are specialized glia controlling osmotic and ionic homeostasis in the retina, in a similar fashion as astrocytes in the brain [11–13]. Important functions attributed to Müller cells include potassium buffering in the retina. In this process, the potassium siphoning in blood vessels and in the vitreous humor through inwardly rectifying potassium channels 4.1 (Kir4.1) [14] is a major mechanism maintaining K^+ ions at a relatively low concentration in the extracellular space. In addition, the water flow through aquaporin 4 (AQP4) channels at the perivascular and end-foot membrane of Müller glia prevents retinal edema [15]. Dystrophin 71 (Dp71) is a scaffolding cytoskeleton molecule required for Kir4.1 and AQP4 channel clustering at the glial cell membrane in the dystrophin-associated protein (DAP) complex [16,17]. The trafficking of Kir4.1 and AQP4 and their targeting to specialized membrane microdomains are incompletely understood. The expression and clustering of Kir4.1 at the plasma membrane is independent on AQP4 [15]. In addition, Kir4.1 and AQP4 location are differently affected by the deletion of Dp71 [18] and by retinal injury [19,20], suggesting the existence of distinct regulatory processes controlling Kir4.1 and AQP4 distribution in the cell. Distinct mechanisms may thus control Kir4.1 and AQP4 expression and location in glial cells.

The enrichment of Nogo-A in Müller cells [5,9] may facilitate the study of its function in glial cell physiology. In the present study, we postulated that the polarized distribution of Nogo-A in Müller cell end-feet may be indicative of its association with proteins of the DAP complex such as Kir4.1. To evaluate the influence of Nogo-A on the distribution and the expression level of Kir4.1, AQP4, Dp71 and β-dystroglycan, we increased the level of Nogo-A in Müller cells with an adenovirus containing Nogo-A cDNA. Adenoviruses specifically transduced Müller cells in the mouse retina *in vivo* [21]. Adenovirus-induced Nogo-A upregulation enhanced Kir4.1 immunoreactivity in the radial processes of Müller glia. In freshly isolated Müller cells from Nogo-A KO mice, potassium conductance was not significantly different from that recorded in Wild-Type (WT) cells. Our data show that Nogo-A overexpression can selectively influence the distribution of Kir4.1 in Müller glia without affecting that of APQ4 or Dp71. Our results further suggest that Nogo-A may participate in the relocation of Kir4.1 that has been reported after injury such as ischemia-reperfusion.

2. Material and methods

2.1. Animals

All animal manipulations were performed in 2–4 month old male C57BL/6 mice. The protocol was approved by the Committee at the *Kantonales Veterinäramt Zürich* of the University of Zürich (Switzerland, permit number #158-2013). All surgeries were performed under isoflurane anesthesia followed by an injection of buprenorphine. Sacrifice was done under isoflurane and an overdose of pentobarbital (Esconarkon). All efforts were made to minimize suffering. Nogo-A KO mice were obtained by homologous recombination of exons 2 and 3 in *Nogo-A* gene in a C57BL/6 genetic background [6].

2.2. Adenovirus production and intraocular injection

The AdEasy system (Agilent) was used to produce the AdNogo-A and AdLacZ adenoviruses. Briefly, the full-length Nogo-A gene was cloned into the AdEasy shuttle vector. The LacZ Shuttle vector was provided by the company. These shuttle plasmids were digested with *Pme*I and purified. BJ5183 bacterial cells were electroporated with either of the linearized shuttle plasmids and the pAdEasy vector to create a recombined larger plasmid. These large plasmids were amplified in XL10 Gold bacteria and purified. Linearization of the plasmids was done with the restriction enzyme PacI. Transfection of the linearized plasmids into mammalian AD-293 cells was performed using Lipofectamine Plus (Invitrogen). Preparation of primary virus stocks was done according to the AdEasy manual (Agilent). A high titer stock of both the AdNogo-A and AdLacZ adenoviruses was done using twenty 100-mm plates of AD-293 plates infected at a MOI of 5. After two days cells began rounding and were harvested, centrifuged and resuspended in PBS. Four cycles of freeze/thaw/vortex were performed. The solution was centrifuged at 7000*g* for 5 min at 4 °C to remove cellular debris. Virus was purified from the solution using a cesium chloride density gradient.

2.3. Intraocular injection of adenoviruses

In order to infect Müller cell with adenoviral vectors, 2 μl of viruses (~10^{10} ip/mL) were intraocularly injected using a 10-μl Hamilton syringe adapted with a pulled-glass tip as previously described [9,22–24]. To allow virus diffusion in the vitreous liquid, the needle was kept in place for ~2 min and then slowly removed to limit the occurrence backflow. Care was taken not to damage the lens during the injections to avoid inflammatory reaction [25–27]. Optimal transgene expression *in vivo* was reached 3 days after adenovirus injections. At this time, mice were intracardially perfused with paraformaldehyde 4% for tissue fixation and retinae were processed for histological analysis.

2.4. Retinal immunostaining

Mice were euthanized with an overdose of anaesthetics and perfused intracardially with PBS and 4% PFA. Eyes were dissected by removing the cornea and the lens from the eyecup. For retinal cross sections, eye cups were post-fixed in 4% PFA overnight at 4 °C. The tissues were then cryoprotected in 30% sucrose and frozen in OCT compound (Tissue-TEK, Sakura, Torrance, CA, USA) with a 2-methylbutane bath cooled with liquid nitrogen. Retinal sections were cut (14 μm) with a cryostat microtome. Immunofluorescent stainings were performed in a blocking solution (5% of normal goat serum or 5% BSA, 0.3% Triton-X-100 in PBS). Primary antibodies were applied overnight at 4 °C and after PBS washes, sections were incubated with the appropriate secondary antibody for 1 h at room temperature. The slides were mounted in Mowiol anti-fading solution (10% Mowiol 4–88 (Calbiochem, Cambridge, UK) in 100 mM Tris, pH 8.5, 25% glycerol and 0.1% DABCO). Primary antibodies were: mouse anti-glutamine synthase (1:200–1:400; Millipore, Zug, Switzerland), rabbit anti-Nogo-A (1:200; Laura/Rb173A [28]), rabbit anti-Kir4.1 (1:200; Alomone, Jerusalem, Israel), rabbit anti-AQP4 (1:200; Millipore), and mouse anti-dystrophin (1:500; Sigma-Aldrich, Buchs, Switzerland). Immunofluorescent labellings were analyzed with a Leica SP2/5 confocal microscope at 40X.

2.5. Western blot analysis

After cervical dislocation, retinae and optic nerves were quickly isolated in Eppendorf tubes and snap frozen in liquid nitrogen. Tissues were kept at −80 °C until protein extraction in CHAPS (0.5%)

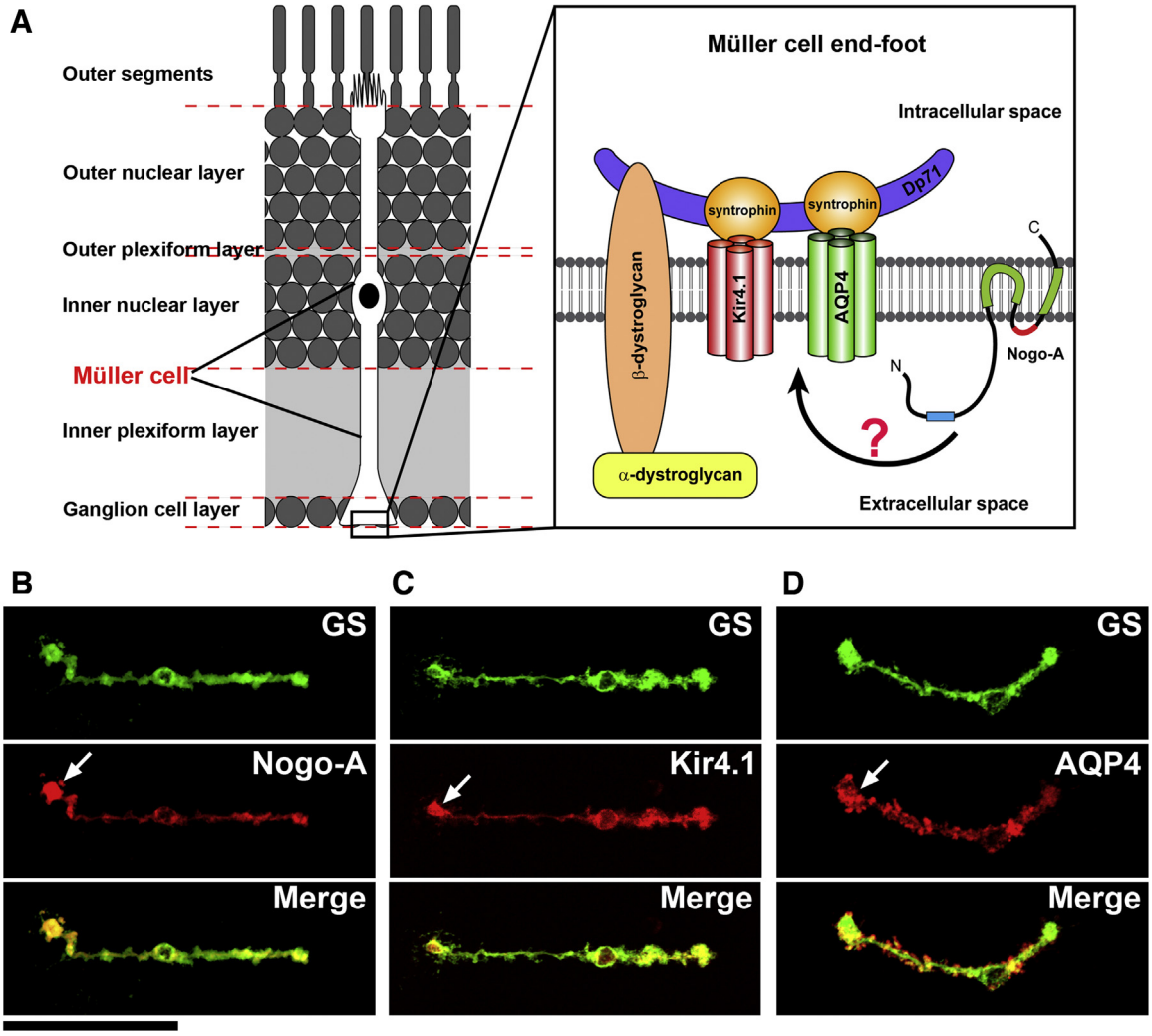

Fig. 1. Nogo-A is enriched in Müller cell end-feet. (A) Working model of dystrophin-associated protein (DAP) assembly in Müller cell end-foot membrane. Kir4.1 and AQP7 clustering at the membrane depends on molecular interactions with Dp71 at the perivascular membrane and end-foot membrane and binding with actin cytoskeleton. Polarization of Nogo-A in the end-foot of Müller glia suggests potential interaction with members of DAP. (B–D) The expression of Nogo-A and DAP proteins was examined by immunofluorescence in isolated mouse Müller cells. (B) Nogo-A was more abundant in the end-foot of Müller glia compared with the glutamine synthase enzyme that was evenly distributed in the cytosol. The inwardly rectifying potassium channel Kir4.1 (C) and aquaporin 4 (AQP4) (D) were also more concentrated in glial cell end-feet. Scale bar = 50 μm.

lysis buffer containing protease inhibitors (Complete mini, Roche Diagnostics; Indianapolis, IN, USA). The samples were fully homogenized and let on ice for 60 min. After centrifugation for 15 min at 15,000*g*, 4 °C, supernatants were collected and used to assess protein concentration (RC DC Protein Assay; Bio-Rad Laboratories, Richmond, CA, USA). Retinal proteins (20 μg/lane) were separated by electrophoresis on 4–12% polyacrylamide gels and transferred to nitrocellulose membranes. Blots were incubated in a blocking solution of 5% bovine serum albumin in 0.2% TBST (0.2% Tween-20 in Tris-base 0.1 M, pH7.4) for 1 h at room temperature, then incubated with primary antibodies overnight at 4 °C. After 3 washings in TBST, the membranes were incubated with horseradish peroxidase-conjugated anti-mouse or anti-rabbit secondary antibodies (1:10,000-1:25,000; Pierce Biotechnology; Rockford, IL, USA). Primary antibodies were mouse anti-GAPDH (1:20,000, Abcam; Cambridge, UK), mouse anti-Nogo-A (1:500, 11C7 [28]), rabbit anti-Nogo-A/B (1:200, Bianca/Rb1 [28]), rabbit anti-Nogo-A (1:200, Laura/Rb173A [28]), mouse anti-glutamine synthase (1:400; Millipore), rabbit anti-Kir4.1 (1:200; Alomone) and rabbit anti-AQP4 (1:200; Millipore), and mouse anti-dystrophin (1:500; Sigma-Aldrich). Protein bands were detected by adding SuperSignal West Pico Chemiluminescent Substrate (Pierce Biotechnology) and after exposure of the blot in a Stella detector. The quantification of the band intensity was done with the ImageJ software (NIH, Bethesda, MD, USA).

2.6. Müller cell cultures

Müller cells were prepared from 2-month old C57BL/6 mice as previously described [9]. Retinae were rapidly dissected in CO2-independent medium after cervical dislocation and rinsed twice in Ringer solution. To dissociate retinal cells, retinae were then incubated in a solution containing 1.5 mg/ml of papain activated by 12.5 mM of L-cystein in a buffer of Ringer. To detach and put cell in suspension, retinae were triturated with a fire-polished Pasteur pipette in a solution of Dulbecco's modified Eagle's medium (DMEM) containing 10% FBS, 0.1 mg/m; DNase I. Müller cells were then separated from other retinal cells on a 0–30% gradient of percoll [29]. Cell were then transferred to a plastic plate. For immunostaining, cells were fixed for 30 min by adding 4% PFA 1hr after plating, rinsed 3 times in PBS and incubating for 1 h in a blocking solution (0.1 M PBS, 0.1% triton-X100, 5% normal

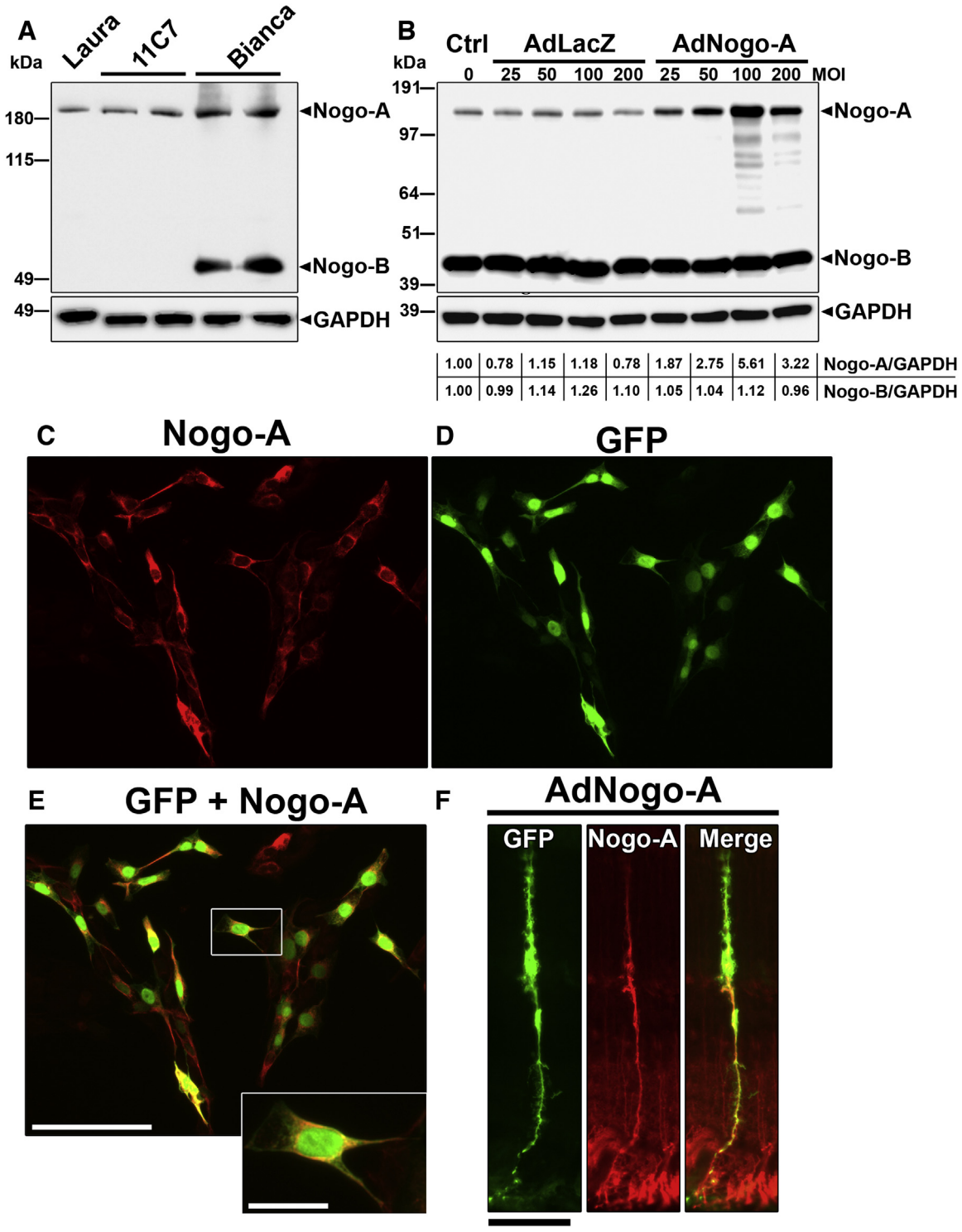

Fig. 2. Adenovirus-mediated Nogo-A upregulation in Müller cells *in vitro* and *in vivo*. (A) In culture, Rat Müller cell line 1 (rMC1) cells expressed Nogo-A and Nogo-B that could be detected with different antibodies recognizing Nogo-A specific domains (11C7 and Laura) or an amino acid sequence shared by Nogo-A and Nogo-B (Bianca). (B) The addition of adenoviruses containing the cDNA of Nogo-A (AdNogo-A) enhanced the protein expression of Nogo-A without affecting the level of Nogo-B. Adenovirus containing the cDNA of LacZ (AdLacZ) was used as a control virus. AdNogo-A (C) increased the immunofluorescent signal of Nogo-A in rMC-1 cells which infection was reflected by GFP reporter detection (D). Nogo-A and GFP superimposition showed that highly infected cells exhibited the highest level of Nogo-A. Higher magnification pictures showed that Nogo-A was located in the endoplasmic reticulum (close-up). *In vivo*, 3 days after intravitreal injection of AdNogo-A, infected GFP-positive Müller cell shows a widespread distribution of Nogo-A in radial processes in contrast to neighbour glia where the protein was restricted to the end-foot of the cells. Scale bars: E = 100 μm, close-up = 25 μm; F = 50 μm.

goat serum). For primary antibody incubation, rabbit anti-Nogo-A (1:200, Laura/Rb173A [28]), mouse anti-glutamine synthase (1:400; Millipore), rabbit anti-Kir4.1 (1:200; Alomone) and rabbit anti-AQP4 (1:200; Millipore), and mouse anti-dystrophin (1:500; Sigma-Aldrich) were added 1 h at room temperature. After washings and secondary antibody incubation, immunofluorescent stainings were imaged by confocal microscopy.

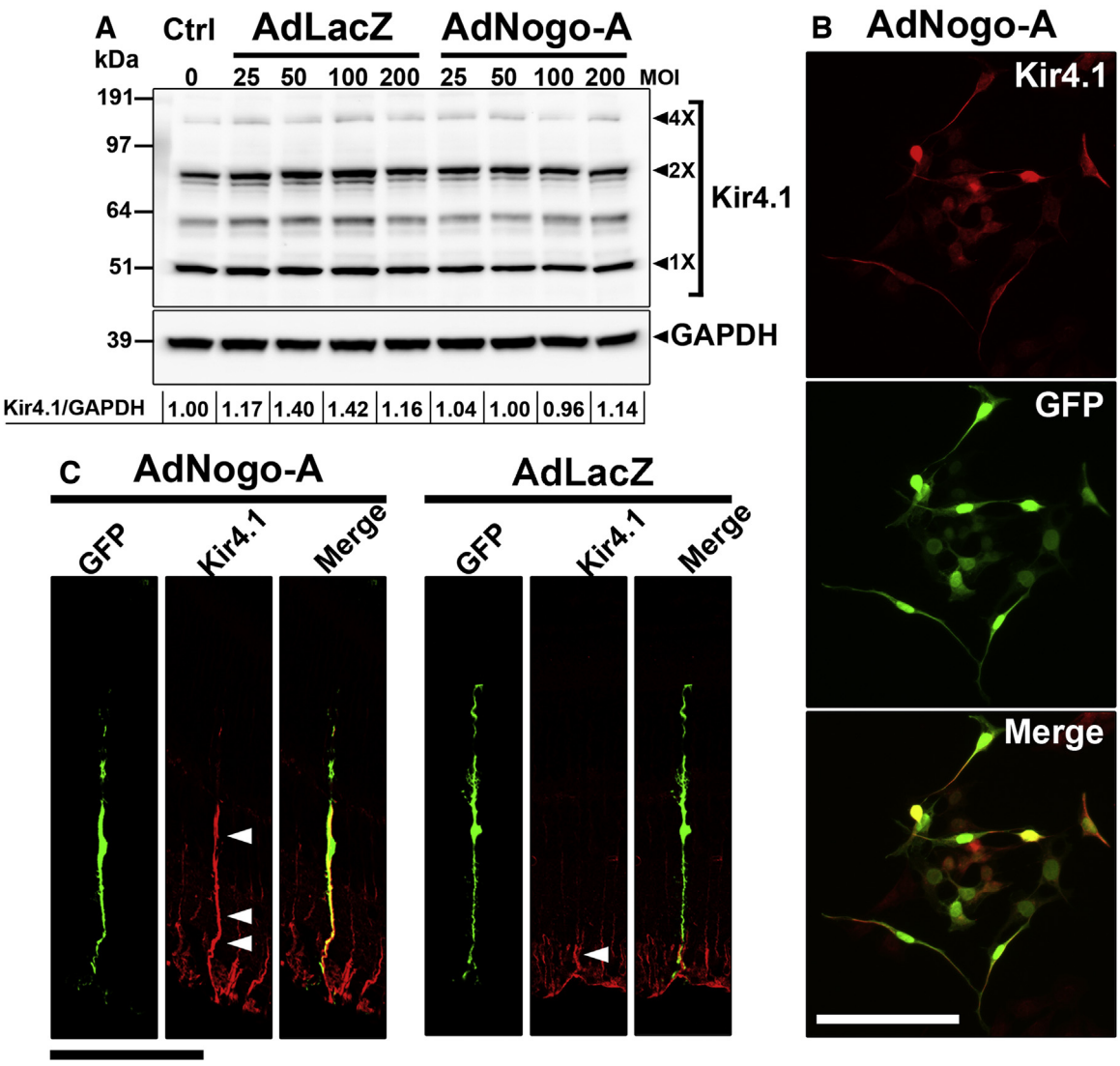

Fig. 3. Adenovirus-mediated Nogo-A upregulation changes the distribution of Kir4.1 in Müller radial glia. The expression and distribution pattern of Kir4.1 was monitored by immunofluorescence and Western blotting in rMC-1 cultures and in retinal crossections 3 days after adenovirus infection. (A) Ectopic increase in Nogo-A expression with AdNogo-A did not influence the level of Kir4.1 detected by Western blotting. (B) However, by immunofluorescence, AdNogo-A enhanced Kir4.1 signal in GFP-positive rMC1 cells. In contrast, Müller cell infection with control AdLacZ vector failed to increase Kir4.1. (C) In a similar fashion, AdNogo-A induced a striking elevation of Kir4.1 immunofluorescent signal in isolated Müller cells *in vivo* relative to AdLacZ (arrow heads). Pictures in C represent optical sections imaged using a confocal microscope. Scale bars = 100 μm.

The rat Müller glia cell line (rMC-1) was also used in this study and was generously provided by the laboratory of Dr Sarthy (Northwestern University, Chicago, USA, IL). Cells were cultured in Dulbecco's modified Eagle's medium (DMEM; Life Technologies) supplemented with 10% fetal bovine serum (FBS; Life Technologies).

2.7. Immunoprecipitation

Mouse retinae were placed on ice and washed with cold PBS. One ml of CHAPS lysate buffer was added (50 mM NaH_2PO_4 pH 8.0, 150 mM NaCl, 0.5% CHAPS, 1 mM PMSF and one mini-EDTA protease inhibitor tablet (Roche) per 7 ml of solution), and the homogenates were incubated on ice for 30 min, tilting every 10 min. Then, the lysates were placed in a cold microfuge tube. The tube was spun at 10,000*g* for 10 min at 4 °C. The supernatant was transferred to a new cold microfuge tube. One microliter of a Sheep anti-Nogo antibody was added to the tube and it was incubated in the cold rotating end-over-end for two hours. Fifty microliters of Protein G (Pierce) was added and the tube was incubated overnight in the cold rotating end-over-end. The tubes were then briefly centrifuged and washed with 1 ml of the following cold buffers: 1× with CHAPS lysis buffer, 3× with Buffer A (10 mM Tris pH 7.5, 150 mM NaCl, 2 mM EDTA and 0.2% NP40), 2× with Buffer B (10 mM Tris pH 7.5, 500 mM NaCl, 2 mM EDTA and 0.2% NP40) and 1× with Buffer C (10 mM Tris pH 7.5). The supernatant was aspirated from the beads with a 27-gauge needle. Beads were resuspended in 50 ul of a 1× SDS loading buffer and boiled for 5 min. After a brief centrifugation, 20 microliters of the buffer solution was loaded on a SDS-PAGE gel.

2.8. Müller cell whole-cell patch-clamp recordings

To perform whole-cell patch-clamp recordings, Müller cells were transferred to a microscope recording chamber and superfused with an extracellular recording solution that contained 125-mM NaCl, 25-mM NaHCO3, 2.5-mM KCl, 1.25-mM NaH2PO4, 1-mM MgCl2, 2-mM CaCl2, 25-mM glucose, and was bubbled with 95% O2/5% CO2 (pH 7.4). Whole cell patch clamp record-

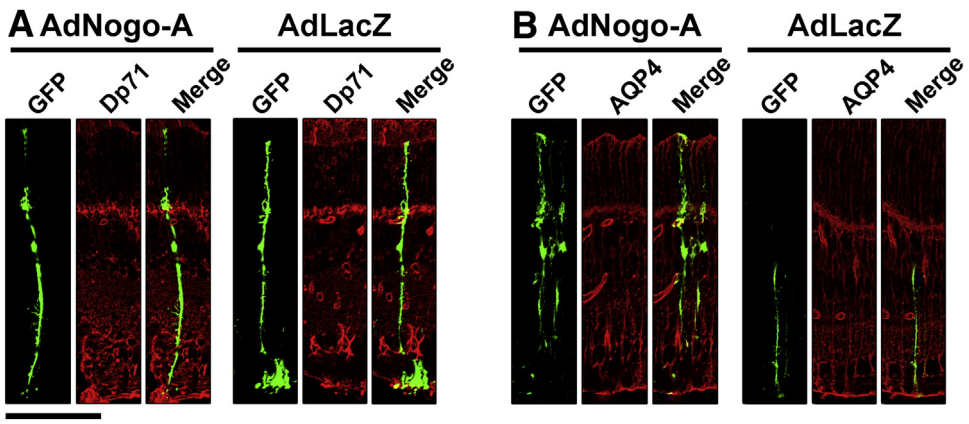

Fig. 4. Adenovirus-mediated Nogo-A upregulation does not change the distribution of dystrophin-associated proteins Dp71 and AQP4 in Müller radial glia. Nogo-A overexpression did not increase Dp71 (A) or AQP4 (B) in Müller cell extensions after AdNogo-A injections in mouse vitreous. Scale bar: 100 μm.

ings were made in voltage clamp mode at near-physiological temperature of 32–36 °C. Before patching Müller cells were visualized at low magnification (5×) under bright-field illumination, and selected for patching using an Olympus upright microscope, fitted with a 40 × /0.8 numerical aperture water-immersion objective (Olympus). Recording pipettes (4–6 MΩ) were pulled from borosilicate glass and filled with (in mM): 135 K-gluconate, 10 Phosphocreatine-Na, 4 KCl, 0.3 Na-GTP, pH 7.2 (adjusted with KOH). Currents were recorded in Müller cells using an Axon Instrument amplifier (Axoclamp-2B), low-pass filtered at 3 kHz and sampled at 10–50 kHz. The recording and stimulation protocols were designed to measure the voltage/current ratio in Müller cells (VI curve). Our stimulation protocol consisted of 10 increasing voltage steps that were applied after a 1 s offset for a brief period of 500 ms. The recording length for each stimulation was 2 s.

3. Results

3.1. Nogo-A is enriched in Müller cell end-feet

We hypothesized that Nogo-A may interact with DAP proteins such as Kir4.1 and AQP4 in Müller cell end-feet (Fig. 1A). To compare their distribution pattern, Nogo-A, Kir4.1 and AQP4 were examined by immunofluorescence in freshly isolated Müller glia (Fig. 1B–D). Glutamine synthase (GS) was used as a specific marker to visualize Müller cells processes. Typically, GS is a glutamate detoxifying enzyme that is evenly present in the cytoplasm of Müller cells [13]. Double immunostaining experiments revealed that Nogo-A was abundant in the end-feet of GS-positive cells (Fig. 1B). Similar distributions were observed for Kir4.1 (Fig. 1C) and AQP4 (Fig. 1D).

3.2. Adenovirus-mediated Nogo-A upregulation in Müller cells in vitro *and* in vivo

We then wondered if Nogo-A influenced the expression of Kir4.1 and AQP4 in Müller cells. In order to address this question, Müller cells were infected *in vitro* and *in vivo* with an adenovirus containing the cDNA of Nogo-A. For Western blot analysis, we infected Rat Müller cell line 1 (rMC-1) [30] cells with adenoviruses. This cell line can be infected at a high rate with adenoviruses [31]. Specific antibodies recognizing Nogo-A (Laura and 11C7) or Nogo-A and Nogo-B (Bianca) allowed to confirm that Nogo-A and Nogo-B are endogenously expressed in rMC-1 cells (Fig. 2A) [28]. The infection of rMC-1 cells with increasing concentrations of AdNogo-A enhanced the level of Nogo-A in a dose-dependent manner without affecting the level of Nogo-B (Fig. 2B). A maximum of Nogo-A expression was reached at multiples of infection (MOI) of 100–200 (see material and methods). Similarly to what we have previously observed for Müller cells in retinal lysates [9], the level of Nogo-B was higher than that of Nogo-A in rMC-1 cells. In these cells, the immunofluorescent staining of Nogo-A showed a stronger protein expression after AdNogo-A infection (Fig. 2C). In this case, infected cells were detected by following the expression of GFP reporter protein (Fig. 2D). The superimposition of the GFP and Nogo-A labelling (Fig. 2E) strongly suggests that the bulk of Nogo-A was intracellular. *In vivo*, 3 days after AdNogo-A infection, Nogo-A appeared throughout the radial process of Müller cells while endogenous Nogo-A was restricted to the end-feet in non-infected glia (Fig. 2F) [9]. Together, these results suggest that AdNogo-A can selectively upregulate Nogo-A in Müller cell bodies.

3.3. Nogo-A overexpression changes the distribution of kir4.1 in Müller radial glia

The level and distribution pattern of Kir4.1 were examined in Müller cells after adenovirus-mediated Nogo-A overexpression *in vitro* and *in vivo*. By Western blot analysis, Nogo-A overexpression did not significantly change Kir4.1 protein expression in rMC-1 cells compared with AdLacZ (Fig. 3A). However, by immunofluorescence, Kir4.1 signal appeared brighter in cells infected with AdNogo-A and expressing GFP reporter protein (Fig. 3B). *In vivo*, AdNogo-A-infected Müller cells displayed a diffused immunoreactivity for Kir4.1 in their radial extensions, in stark contrast with control cells infected with AdLacZ where Kir4.1 expression is concentrated at the end-foot (Fig. 3C). To determine if the effect of Nogo-A overexpression affected other proteins belonging to the dystrophin-associated protein complex, Dp71 and AQP4 were labelled in infected retinae (Fig. 4). Neither Dp71 (Fig. 4A) nor AQP4 (Fig. 4B) exhibited a diffused distribution in GFP-positive Müller cells after their infection with AdNogo-A or AdLacZ. These observations tend to show that Nogo-A overexpression specifically leads to ectopic distribution of Kir4.1 along radial glial processes without affecting its level of expression.

3.4. Nogo-A and kir4.1 interacts in Müller glia

To determine if Nogo-A and Kir4.1 molecules were bound *in vivo*, co-immunoprecipitation experiments were carried out with mouse retinal lysates. The retinae from three different mice were used to immunoprecipitate Nogo-A with a sheep antibody [28] whereas negative controls were obtained by adding control sheep IgG to retinal lysates from 3 other animals. The tetrameric form of Kir4.1 (~180 kDa) was detected after Nogo-A immunoprecipitation while no signal could be observed using control sheep IgG (Fig. 5A). We

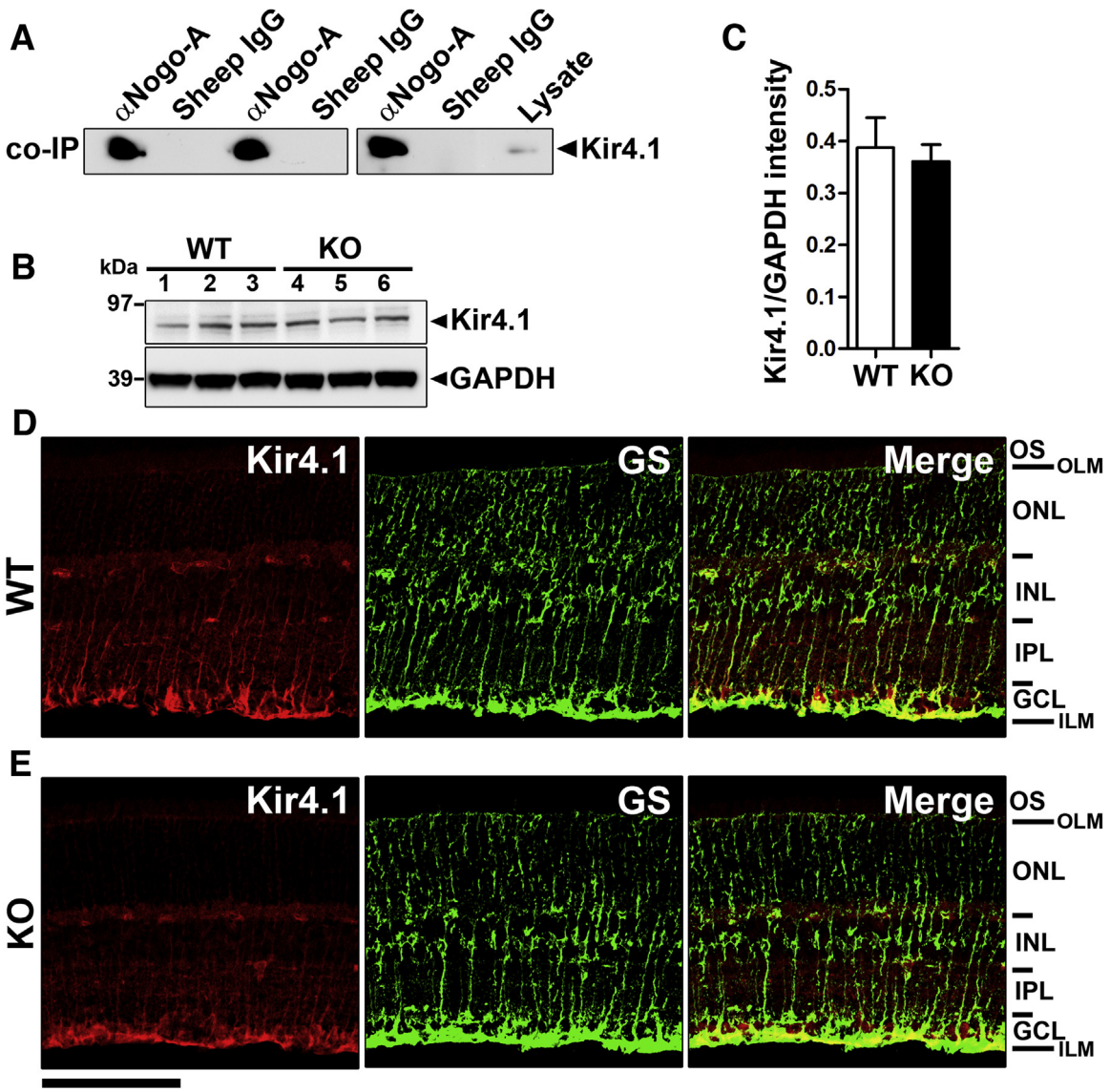

Fig. 5. Nogo-A interacts with Kir4.1 in Müller glia. (A) In retinal lysates Kir4.1 co-immunoprecipitated along with Nogo-A after sheep anti-Nogo-A addition while control sheep antibody did not allow to detect Kir4.1. Each lane represents 2 retinae from the same animal. (B) In Nogo-A KO retinae, the level of Kir4.1 did not differ from that in WT mice as quantitatively determined by densitometry analysis of Kir4.1 (mean ± S.E.M., n = 3 mice/group) (C). D) Immunofluorescent staining of Kir4.1 and GS in WT and Nogo-A KO retinal sections. In WT retinae, Kir4.1 staining was brighter in Müller perivascular membrane and end-feet that in Nogo-A KO mice. Glutamine synthase antibody evenly stained radial Müller glia processes stretched between the inner limiting membrane (ILM) and outer limiting membrane (OLM). Scale bar = 100 μm.

then wondered if endogenously expressed Nogo-A influenced the expression of Kir4.1 in Müller cell end-feet. To address this question, we followed Kir4.1 by Western blotting (Fig. 5B, C) and by immunofluorescence on Nogo-A KO and WT mouse retinal sections (Fig. 5D, E). Nogo-A KO mice have been characterized before [5,6,9]. By Western blotting, the level of Kir4.1 did not appear different between Nogo-A KO and WT retinae. Moreover, the immunofluorescent signal of Kir4.1 was visualized in the perivascular processes of Müller cells and at their end-feet adjacent to the vitreous body, in Nogo-A KO and WT Müller glia extensions (Fig. 5D, E). Other proteins of the same macromolecular complex, such as Dp71 or AQP4 were not affected by Nogo-A gene deletion (Fig. 6); in WT and Nogo-A KO mice, AQP4 and Dp71 (Fig. 6A) were localized in the end-feet and perivascular Müller cell processes in a consistent manner with what has been described before [32,33]. The protein expression of Dp71 and β-Dystroglycan (Fig. 6B–C) was not significantly different between WT and KO mice (n = 3 mice/group, Student's *t*-test: $p > 0.05$).

3.5. Potassium conductance is not altered in Müller glia-deprived of Nogo-A

The conductance of potassium through Kir4.1 has a strong influence on the resting membrane potential of Müller cells. In the absence of Kir4.1, the membrane potential is depolarized [33]. We sought to assess whether Nogo-A gene deletion affected Kir4.1-dependent inward and outward flows of potassium in whole cell preparations. As described before, Müller cells were isolated from WT and Nogo-A KO adult mouse retinae. Shortly after Müller cell plating, *i.e.* 1–3 h after retinal cell dissociation, current intensities were registered at voltages ranging from −130 mV to +60 mV (Fig. 7A). In order to confirm the role of potassium in currents measurements, the potassium channel blocker $BaCl_2$ was added to the same cell (Fig. 7B). The addition of $BaCl_2$ resulted in an almost complete abolition of K^+ conductance, confirming that current changes recorded in Müller cells are generated by the flow of K^+ through the membrane. Plotting I–V curves showed very similar current

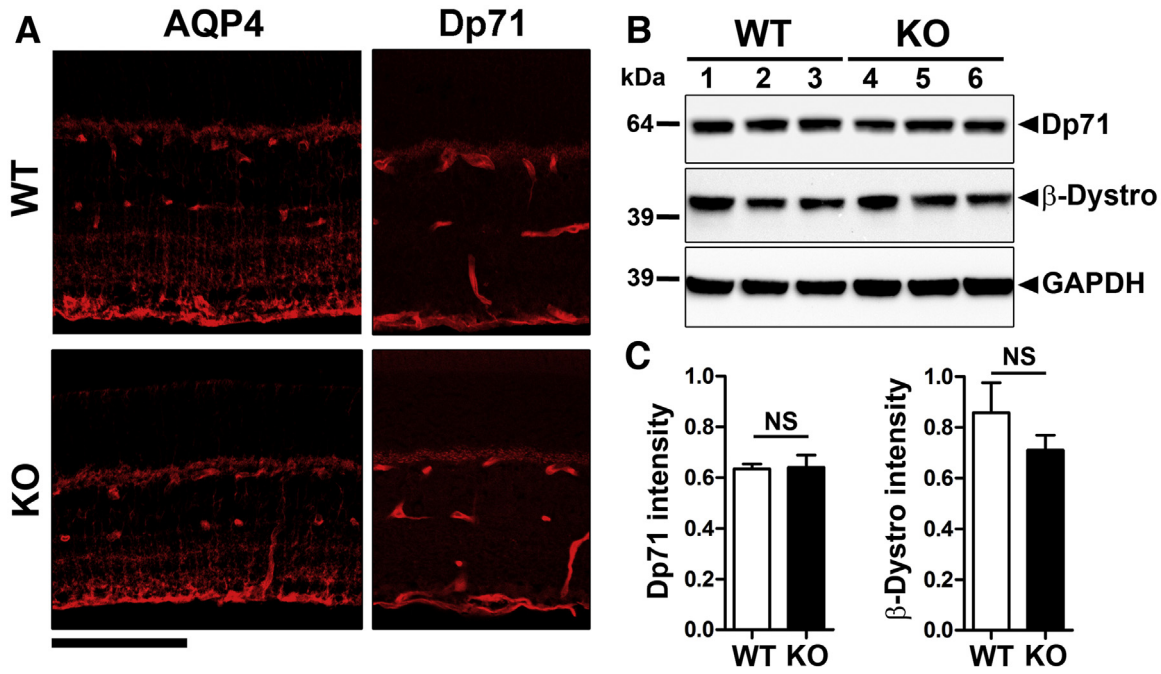

Fig. 6. Expression of dystrophin-associated proteins in Nogo-A KO retinal crossections. (A) The distribution pattern of Dp71 and AQP4 was analyzed by immunofluorescence in Nogo-A KO and WT mouse retinal crossections. The localization of the 2 proteins was not different in the end-feet and perivascular Müller cell processes. (B) By Western blotting, the protein expression of Dp71 and β-Dystro was similar between the 2 experimental groups. (C) Densitometric quantification of Western blots did not reveal significant variation in WT compared with KO mice (n = 3 mice/group, Student's *t*-test: $p > 0.05$).

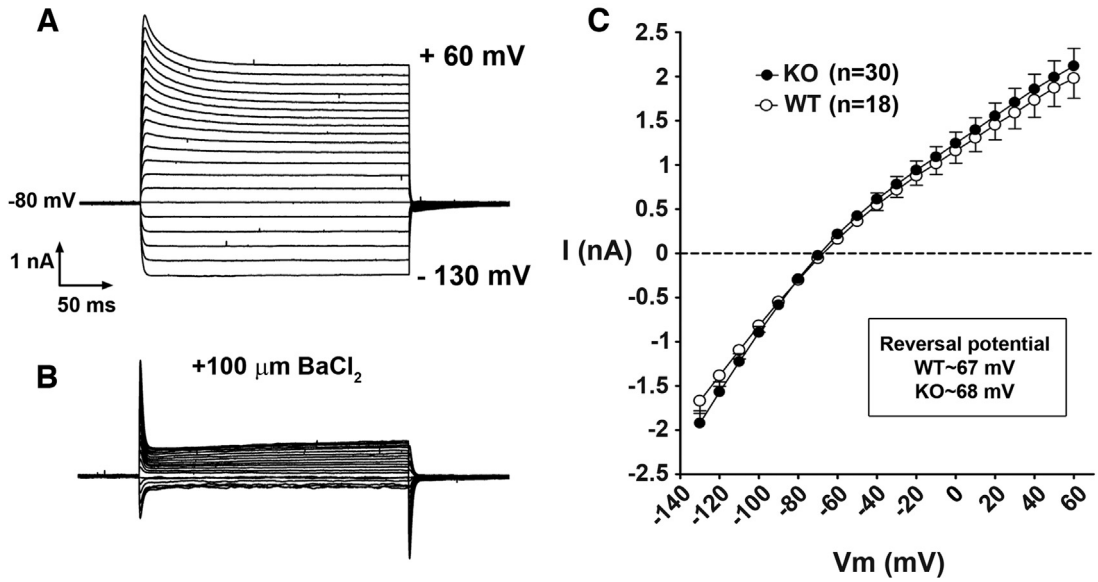

Fig. 7. Potassium conductance is not modified in Müller cells deprived of Nogo-A. (A) Potassium currents were recorded by patch-clamping in isolated Müller cells for voltages ranging from −130 mV to +60 mV. (B) The addition of potassium channel blocker $BaCl_2$ to the same cell drastically reduced voltage-induced current changes, confirming that the current recorded in Müller cells stemmed from K^+ conductance. (C) I–V curves showed very similar variations in WT as in Nogo-A KO cells. The reversal potential measured in WT cells (~67 mV, n = 18) was comparable to that recorded in Nogo-A KO cells (~68 mV, n = 30).

intensity changes in response to voltage changes in WT as in Nogo-A KO cells. On average, the reversal potential calculated in WT cells (n = 18) was ~67 mV compared with ~68 mV in Nogo-A KO cells (n = 30) (Fig. 7C). These values are in agreement with previous measurements [15]. These data suggest that K^+ conductance is not altered in Müller cells after Nogo-A gene deletion.

4. Discussion

In this study, we observed that the reticulon protein Nogo-A/RTN4A and Kir4.1 coexisted in the inner processes of Müller cells. Adenovirus-mediated Nogo-A overexpression selectively enhanced the immunofluorescent signal of Kir4.1 in Müller cell extensions *in vivo*. *In vitro*, the expression level of Kir4.1 protein was not modified after rMC-1 cell infection with AdNogo-A

compared with AdLacZ. Increased Kir4.1 immunoreactivity may thus be attributable to subcellular redistribution of this potassium channel rather than to protein synthesis upregulation. Co-immunoprecipitation results revealed molecular interactions between Nogo-A and Kir4.1. In addition, deleting Nogo-A gene in KO mice did not modify the expression pattern of Kir4.1 and potassium conductance in Müller glia.

4.1. Nogo-A is associated with kir4.1 in Müller glia end-feet

The enrichment of Nogo-A in Müller cell end-feet along with proteins of the DAP complex such as Kir4.1 was very striking. Our co-IP data confirmed that Nogo-A and Kir4.1 interacted together. The binding between Kir4.1 and Nogo-A may explain the increase in Kir4.1 immunoreactivity that was detected in Müller cell radial extensions after infection with AdNogo-A. Surprisingly, the distribution of AQP4 and Dp71 remained unchanged while these 2 proteins are known to be part of a macromolecular complex together with Kir4.1. However, Kir4.1 and AQP4-Dp71 can exist in distinct dystrophin microdomains [18]; it has been proposed that utrophin could associate with Kir4.1 (Kir4.1a) at the plasma membrane in a similar fashion as Dp71, when Dp71 gene is ablated. Therefore, according to this model, Kir4.1 may exist in 2 molecular complexes that may or may not contain Dp71-AQP4. It will be important to determine if Nogo-A and Kir4.1 associate in a molecular complex comprising β-dystroglycan and utrophin to better define the molecular interactions of Nogo-A in Müller glia [18].

4.2. Kir4.1 localization is altered in Nogo-A-overexpressing Müller cells

By immunofluorescence, Kir4.1 appeared brighter after Müller cell transduction with AdNogo-A whereas the level of Kir4.1 protein expression was not modified by Western blotting. The elevation of Kir4.1 immunoreactivity may result from the accumulation of Kir4.1 in restricted regions of the cell, in the endoplasmic reticulum or at the plasma membrane. It has previously been shown that Kir4.1 immunoreactivity was decreased at the end-feet and perivascular membrane of Müller cells lacking Dp71 while its expression level turned out to be unchanged by Western blotting [16,17]. In this situation, the loss of intense Kir4.1 immunoreactivity around blood vessels and in end-feet is caused by its even distribution at the plasma membrane along Müller cell extension. Interestingly, the loss of concentrated Kir4.1 at the end-foot and perivascular membrane does not induce a change in potassium conductance measured in the whole cell [16,17]. Similarly, Nogo-A may change the subcellular localization of Kir4.1 channels in glial cells but may not influence their ability to conduct potassium current. This hypothesis could not be tested after Nogo-A overexpression since only a small number of Müller cells can be transduced by adenoviruses *in vivo* [21]. In addition, infecting Müller cells in culture was not an alternative to follow potassium currents; in *in vitro* conditions, Müller cells quickly lose their potassium conductance as a result of Kir4.1 internalization [34]. However, using new viral vectors such as engineered adeno-associated viruses called ShH10 [22,35], it will be possible to determine the effect of Nogo-A overexpression on potassium flow across the Müller cell membrane after the isolation of cells infected *in vivo*.

4.3. The role of reticulons in Müller glia

By electrophysiology, we observed that potassium conductance in Müller glia did not depend on Nogo-A expression. The membrane potential of Nogo-A KO Müller cells was not different from that measured in WT cells. This suggests that Nogo-A expression is not required for potassium conductance. However, other reticulons could compensate for the lack of Nogo-A in Müller cells. RTN3 and RTN4B/Nogo-B are highly expressed in Müller cells where their level could exceed that of Nogo-A [9,10,36]. The high level of reticulon expression in Müller cells is intriguing. It has been shown that reticulons like Nogo-A generated tubular endoplasmic reticulum by influencing membrane curvature [37,38]. Strikingly, the localization of Nogo-A that we observed in the inner Müller cell extension and end-foot corresponds to a portion of the cell densely packed with smooth endoplasmic reticulum [39,40]. At this place, Nogo-A could therefore contribute to shape and stabilize the endoplasmic reticulum structure.

Molecular interactions mediated by the reticulon homology domain (RHD) may lead to Kir4.1 sequestration in the endoplasmic reticulum. The RHD is a highly conserved sequence of ~180 amino acids in the C-terminal region of Nogo-A, Nogo-B and RTN3 [1]. The RHD contains 2 putative transmembrane regions involved in reticulon binding to the membrane. Importantly, the RHD also mediates the association of reticulons with beta-site APP-cleaving enzyme 1 (BACE1); reticulon1-4 overexpression induces BACE1 retention in the endoplasmic reticulum in a RHD-dependent manner and hence reduces the level of BACE1 at the plasma membrane [41,42]. In a similar fashion, the RHD of Nogo-A might participate in the binding to Kir4.1 and causes its sequestration in the endoplasmic reticulum. The mechanisms regulating Nogo-A trafficking in the cell are not understood yet. Like other RTNs, Nogo-A lacks an N-term signal peptide [2]. However, it has been shown that the N-terminal domain of Kir4.1 was involved in its export from the Golgi compartment to the plasma membrane [43]. Nogo-A colocalizes with Golgi markers as well [44]. Therefore, Nogo-A might change Kir4.1 localization in subcellular compartments, for instance by interfering with the amino domain of Kir4.1. This mechanism may contribute to the loss of Kir4.1 at the plasma membrane that has been associated with a marked potassium conductance reduction in pathological conditions [45].

5. Summary

In this study we observed that Nogo-A was enriched in Müller cell endfeet where it interacts with Kir4.1. Virus-mediated Nogo-A overexpression induced ectopic distribution of Kir4.1 throughout Müller cell extensions, while other proteins of the dystrophin-associated protein complex like AQP4 were not affected. These results show for the first time that proteins of the reticulon family can influence the distribution of Kir4.1 in retinal glial cells. Further work should clarify the role of Nogo-A in Kir4.1 trafficking and function in the healthy retina. The effect that Nogo-A may exert on Kir4.1 function after retinal injury (*e.g.* ischemia) remains to be investigated.

Conflict of interest

The authors declare no conflict of interest.

Acknowledgements

This work was supported by grants from the *Fonds de recherche du Québec-Santé* (FRQS; grant #30633), the Natural Sciences and Engineering Research Council of Canada (NSERC; grant #RGPIN-2015-05084), the Diabetes Québec Foundation and the Eye Disease Foundation in Québec.

References

[1] M.S. Chen, A.B. Huber, M.E. van der Haar, M. Frank, L. Schnell, A.A. Spillmann, et al., Nogo-A is a myelin-associated neurite outgrowth inhibitor and an antigen for monoclonal antibody IN-1, Nature 403 (6768) (2000) 434–439.

[2] T. GrandPre, F. Nakamura, T. Vartanian, S.M. Strittmatter, Identification of the Nogo inhibitor of axon regeneration as a Reticulon protein, Nature 403 (6768) (2000) 439–444.
[3] M.E. Schwab, Functions of Nogo proteins and their receptors in the nervous system, Nat. Rev. Neurosci. 11 (12) (2010) 799–811.
[4] V. Pernet, M.E. Schwab, The role of Nogo-A in axonal plasticity, regrowth and repair, Cell Tissue Res. 349 (1) (2012) 97–104.
[5] V. Pernet, S. Joly, F. Christ, L. Dimou, M.E. Schwab, Nogo-A and myelin-associated glycoprotein differently regulate oligodendrocyte maturation and myelin formation, J. Neurosci. 28 (29) (2008) 7435–7444.
[6] M. Simonen, V. Pedersen, O. Weinmann, L. Schnell, A. Buss, B. Ledermann, et al., Systemic deletion of the myelin-associated outgrowth inhibitor Nogo-A improves regenerative and plastic responses after spinal cord injury, Neuron 38 (2) (2003) 201–211.
[7] L. Montani, B. Gerrits, P. Gehrig, A. Kempf, L. Dimou, B. Wollscheid, et al., Neuronal Nogo-A modulates growth cone motility via Rho-GTP/LIMK1/cofilin in the unlesioned adult nervous system, J. Biol. Chem. 284 (16) (2009) 10793–10807.
[8] A. Kempf, L. Montani, M.M. Petrinovic, A. Schroeter, O. Weinmann, A. Patrignani, et al., Upregulation of axon guidance molecules in the adult central nervous system of Nogo-A knockout mice restricts neuronal growth and regeneration, Eur. J. Neurosci. 38 (11) (2013) 3567–3579.
[9] V. Pernet, S. Joly, D. Dalkara, O. Schwarz, F. Christ, D. Schaffer, et al., Neuronal Nogo-A upregulation does not contribute to ER stress-associated apoptosis but participates in the regenerative response in the axotomized adult retina, Cell Death Differ. 19 (7) (2012) 1096–1108.
[10] A.B. Huber, O. Weinmann, C. Brosamle, T. Oertle, M.E. Schwab, Patterns of Nogo mRNA and protein expression in the developing and adult rat and after CNS lesions, J. Neurosci. 22 (9) (2002) 3553–3567.
[11] A. Bringmann, T. Pannicke, J. Grosche, M. Francke, P. Wiedemann, S.N. Skatchkov, et al., Muller cells in the healthy and diseased retina, Prog. Retin. Eye Res. 25 (4) (2006) 397–424.
[12] E. Newman, A. Reichenbach, The Muller cell: a functional element of the retina, Trends Neurosci. 19 (8) (1996) 307–312.
[13] A. Reichenbach, A. Bringmann, New functions of Muller cells, Glia 61 (5) (2013) 651–678.
[14] E.A. Newman, Regional specialization of retinal glial cell membrane, Nature 309 (5964) (1984) 155–157.
[15] J. Ruiz-Ederra, H. Zhang, A.S. Verkman, Evidence against functional interaction between aquaporin-4 water channels and Kir4.1 potassium channels in retinal Muller cells, J. Biol. Chem. 282 (30) (2007) 21866–21872.
[16] N.C. Connors, P. Kofuji, Dystrophin Dp71 is critical for the clustered localization of potassium channels in retinal glial cells, J. Neurosci. 22 (11) (2002) 4321–4327.
[17] C. Dalloz, R. Sarig, P. Fort, D. Yaffe, A. Bordais, T. Pannicke, et al., Targeted inactivation of dystrophin gene product Dp71: phenotypic impact in mouse retina, Hum. Mol. Genet. 12 (13) (2003) 1543–1554.
[18] P.E. Fort, A. Sene, T. Pannicke, M.J. Roux, V. Forster, D. Mornet, et al., Kir4.1 and AQP4 associate with Dp71- and utrophin-DAPs complexes in specific and defined microdomains of Muller retinal glial cell membrane, Glia 56 (6) (2008) 597–610.
[19] T. Pannicke, I. Iandiev, O. Uckermann, B. Biedermann, F. Kutzera, P. Wiedemann, et al., A potassium channel-linked mechanism of glial cell swelling in the postischemic retina, Mol. Cell. Neurosci. 26 (4) (2004) 493–502.
[20] T. Pannicke, I. Iandiev, A. Wurm, O. Uckermann, F. vom Hagen, A. Reichenbach, et al., Diabetes alters osmotic swelling characteristics and membrane conductance of glial cells in rat retina, Diabetes 55 (3) (2006) 633–639.
[21] A. Di Polo, L.J. Aigner, R.J. Dunn, G.M. Bray, A.J. Aguayo, Prolonged delivery of brain-derived neurotrophic factor by adenovirus-infected Müller cells temporarily rescues injured retinal ganglion cells, Proc. Natl. Acad. Sci. U. S. A. 95 (1998) 3978–3983.
[22] V. Pernet, S. Joly, D. Dalkara, N. Jordi, O. Schwarz, F. Christ, et al., Long-distance axonal regeneration induced by CNTF gene transfer is impaired by axonal misguidance in the injured adult optic nerve, Neurobiol. Dis. 51 (2013) 202–213.
[23] V. Pernet, S. Joly, N. Jordi, D. Dalkara, A. Guzik-Kornacka, J.G. Flannery, et al., Misguidance and modulation of axonal regeneration by Stat3 and Rho/ROCK signaling in the transparent optic nerve, Cell. Death. Dis. 4 (2013) e734.
[24] F. Vajda, N. Jordi, D. Dalkara, S. Joly, F. Christ, B. Tews, et al., Cell type-specific Nogo-A gene ablation promotes axonal regeneration in the injured adult optic nerve, Cell Death Differ. 22 (2) (2015) 323–335.
[25] D. Fischer, P. Heiduschka, S. Thanos, Lens-injury-stimulated axonal regeneration throughout the optic pathway of adult rats, Exp. Neurol. 172 (2) (2001) 257–272.
[26] S. Leon, Y. Yin, J. Nguyen, N. Irwin, L.I. Benowitz, Lens injury stimulates axon regeneration in the mature rat optic nerve, J. Neurosci. 20 (12) (2000) 4615–4626.
[27] V. Pernet, A. Di Polo, Synergistic action of brain-derived neurotrophic factor and lens injury promotes retinal ganglion cell survival, but leads to optic nerve dystrophy in vivo, Brain 129 (4) (2006) 1014–1026.
[28] D.A. Dodd, B. Niederoest, S. Bloechlinger, L. Dupuis, J.P. Loeffler, M.E. Schwab, Nogo-A, −B, and −C are found on the cell surface and interact together in many different cell types, J. Biol. Chem. 280 (13) (2005) 12494–12502.
[29] M.C. Trachtenberg, D.J. Packey, Rapid isolation of mammalian Muller cells, Brain Res. 261 (1) (1983) 43–52.
[30] P.V. Sarthy, Establishment of Muller cell cultures from adult rat retina, Brain Res. 337 (1) (1985) 138–141.
[31] M.D. Shelton, T.S. Kern, J.J. Mieyal, Glutaredoxin regulates nuclear factor kappa-B and intercellular adhesion molecule in Muller cells: model of diabetic retinopathy, J. Biol. Chem. 282 (17) (2007) 12467–12474.
[32] E.A. Nagelhus, M.L. Veruki, R. Torp, F.M. Haug, J.H. Laake, S. Nielsen, et al., Aquaporin-4 water channel protein in the rat retina and optic nerve: polarized expression in Muller cells and fibrous astrocytes, J. Neurosci. 18 (7) (1998) 2506–2519.
[33] P. Kofuji, P. Ceelen, K.R. Zahs, L.W. Surbeck, H.A. Lester, E.A. Newman, Genetic inactivation of an inwardly rectifying potassium channel (Kir4.1 subunit) in mice: phenotypic impact in retina, J. Neurosci. 20 (15) (2000) 5733–5740.
[34] M. Ishii, Y. Horio, Y. Tada, H. Hibino, A. Inanobe, M. Ito, et al., Expression and clustered distribution of an inwardly rectifying potassium channel KAB-2/Kir4.1, on mammalian retinal Muller cell membrane: their regulation by insulin and laminin signals, J. Neurosci. 17 (20) (1997) 7725–7735.
[35] R.R. Klimczak, J.T. Koerber, D. Dalkara, J.G. Flannery, D.V. Schaffer, A novel adeno-associated viral variant for efficient and selective intravitreal transduction of rat Muller cells, PLoS One 4 (10) (2009) e7467.
[36] E. Kumamaru, C.H. Kuo, T. Fujimoto, K. Kohama, L.H. Zeng, E. Taira, et al., Reticulon3 expression in rat optic and olfactory systems, Neurosci. Lett. 356 (1) (2004) 17–20.
[37] G.K. Voeltz, W.A. Prinz, Y. Shibata, J.M. Rist, Rapoport TA: a class of membrane proteins shaping the tubular endoplasmic reticulum, Cell 124 (3) (2006) 573–586.
[38] J. Hu, Y. Shibata, C. Voss, T. Shemesh, Z. Li, M. Coughlin, et al., Membrane proteins of the endoplasmic reticulum induce high-curvature tubules, Science 319 (5867) (2008) 1247–1250.
[39] M. Wakakura, W.S. Foulds, Comparative ultrastructural study of rabbit Muller cells in vitro and in situ, Eye (Lond) 2 (Pt. 6) (1988) 664–669.
[40] A. Reichenbach, Attempt to classify glial cells by means of their process specialization using the rabbit retinal Muller cell as an example of cytotopographic specialization of glial cells, Glia 2 (4) (1989) 250–259.
[41] W. He, X. Hu, Q. Shi, X. Zhou, Y. Lu, C. Fisher, et al., Mapping of interaction domains mediating binding between BACE1 and RTN/Nogo proteins, J. Mol. Biol. 363 (3) (2006) 625–634.
[42] W. He, Q. Shi, X. Hu, R. Yan, The membrane topology of RTN3 and its effect on binding of RTN3 to BACE1, J. Biol. Chem. 282 (40) (2007) 29144–29151.
[43] C. Stockklausner, N. Klocker, Surface expression of inward rectifier potassium channels is controlled by selective Golgi export, J. Biol. Chem. 278 (19) (2003) 17000–17005.
[44] T. Oertle, M.E. van der Haar, C.E. Bandtlow, A. Robeva, P. Burfeind, A. Buss, et al., Nogo-A inhibits neurite outgrowth and cell spreading with three discrete regions, J. Neurosci. 23 (13) (2003) 5393–5406.
[45] E. Ulbricht, T. Pannicke, M. Hollborn, M. Raap, I. Goczalik, I. Iandiev, et al., Proliferative gliosis causes mislocation and inactivation of inwardly rectifying K(+) (Kir) channels in rabbit retinal glial cells, Exp. Eye Res. 86 (2) (2008) 305–313.